Structural Modification of Single-Layer Carbon Nanotubes with an Electron Beam

Ching-Hwa Kiang,*,†,‡ William A. Goddard, III,‡ Robert Beyers,† and Donald S. Bethune†

IBM Research Division, Almaden Research Center, 650 Harry Road, San Jose, California 95120-6099, and Materials and Process Simulation Center, Beckman Institute, Division of Chemistry and Chemical Engineering, California Institute of Technology, Pasadena, California 91125

Received: September 8, 1995; In Final Form: November 16, 1995[⊗]

Transmission electron imaging and diffraction are used to probe the atomic-level structure of single-layer carbon nanotubes. The nanotubes bend, fold, kink, and radially deform. They have a tendency to form parallel bundles of tubes, and this bundling process has been observed in real time. In addition, the electron beam is used to locally cut and anneal nanotubes.

1. Introduction

There have been numerous studies of the synthesis and properties of multilayer carbon nanotubes[1] since the discovery by Iijima in 1991.[2] These tubes form on the cathode tip without a catalyst. They are straight and have multiple concentric layers. Very different nanotubes are produced when transition metal catalysts (*e.g.* Fe, Co, or Ni) are covaporized with carbon. These tubes are single-layered and tend to stick together in parallel bundles. These threadlike bundles and individual tubules are woven into a carbon net, giving rise to a soot with a rubbery texture.[3−7] Despite a wealth of theoretical work on the electronic structure[1,8−13] and the vibrational properties[1,12,14,15] of single-layer nanotubes, investigations of these materials have to date relied heavily on transmission electron microscopy (TEM) imaging and diffraction. A principal difficulty is the separation of nanotubes from fullerene soot particles and amorphous or graphitic carbon material containing embedded metal clusters. TEM, therefore, remains the most powerful general structural tool for studying catalytically grown single-layer carbon nanotubes.

In this paper we use TEM direct imaging and diffraction to probe the atomic-level structure of single-layer nanotubes. In section 2 we describe the experimental procedures for sample preparation. In section 3 we discuss the structure of carbon nanotubes. In section 4 we show that nanotubes can bend, fold, kink, and radially deform. We also demonstrate a real time observation of the nanotube bundling process and the use of an electron beam to locally cut, weld, and anneal nanotubes.

2. Experimental Section

Single-layer nanotubes were prepared with Co catalyst, in a process similar to that described in ref 6. In brief, electrodes were vaporized by a DC arc under 400 Torr of helium flowing at 10−15 mL/min. The electrodes were 6 mm diameter graphite rods, with the anodes drilled out to 4 mm inside diameter and filled with mixtures of C, Co, and heavy metal (*e.g.* Bi and Pb). The metal concentrations used were 4% each for Co and the heavy metal (in atom percent, relative to the carbon). The soot collected from the chamber wall was examined using a Topcon 002B transmission electron microscope (TEM) operating at 100 or 200 kV with a Gatan Model 679 slow-scan camera. Samples were prepared by sonicating soot in ethanol and putting a drop of the suspension onto a holey carbon grid.

3. Structure of Single-Layer Carbon Nanotubes

On the molecular scale, ideal single-layer carbon nanotubes can be thought of either as one-dimensional crystals or as all-carbon semiflexible polymers. Alternatively, one can think of capped nanotubes as giant fullerenes, with micrometer lengths and masses on the order of 10^6 amu.[16] The structure of a perfectly cylindrical section of such a nanotube is specified by only two parameters: the tube diameter D and the tube helicity angle α.[3,17] Both of these parameters can be obtained directly from TEM images and diffraction patterns. Using the microbeam diffraction technique, we obtain a diffraction pattern of a single-layer nanotube of 3.6 nm diameter. The electron beam was operated at an acceleration voltage of 100 kV, and the camera exposure time was set at 32 s to acquire a clear diffraction pattern. The diffraction spots of the nanotube were eventually smeared out by the superposition of a ring pattern characteristic of amorphous carbon. The amorphous carbon deposited on the nanotube was from the surrounding carbon soot evaporated by the electron beam. Figure 1 shows the diffraction pattern and the image of the $D = 3.6$ nm tube that the diffraction pattern was taken from. A helicity angle of $\alpha = 30°$, which corresponds to a nonhelical armchair structure, was obtained from the diffraction pattern in Figure 1. In the notation of ref 8 the tube is designated by the index pair (n, n), with $n = 26$, and it is predicted that such a tube will be metallic.

Nanotubes are often observed to be grossly distorted from ideal straight and cylindrical geometries. While the carbon mesh structure of the tubes is expected to be tough and to endow them with considerable tensile strength[18] and rigidity,[19] the defects in the graphene sheet structure allow the tubes to bend sharply, buckle, and distort radially without tearing. TEM observations suggest that the rigidity of the single-layer tubes depends on their diameter. Small-diameter tubes typically appear to have near-perfect cylindrical shapes, as suggested by their constant projected widths in TEM images. In contrast, large nanotubes (diameter > 2 nm) are often observed to be deformed. Defects often occur when tubes are tangled with each other, as in Figure 2a, where a large tube flattens into a ribbon and twists as it separates from a tube bundle. Folding of tubes was commonly observed, particularly for larger diameter tubes. Figure 2b shows a 3.3 nm diameter tube that folded along the soot, with a rigid 1.5 nm diameter tube nearby. Despite these local defects, the nanotube diameter appears

* Author to whom correspondence should be addressed. Current address: Department of Physics, Massachusetts Institute of Technology, 77 Massachusetts Avenue, Room 13-3037, Cambridge, MA 02139.
† IBM Research Division.
‡ California Institute of Technology.
⊗ Abstract published in *Advance ACS Abstracts,* February 1, 1996.

0022-3654/96/20100-3749$12.00/0

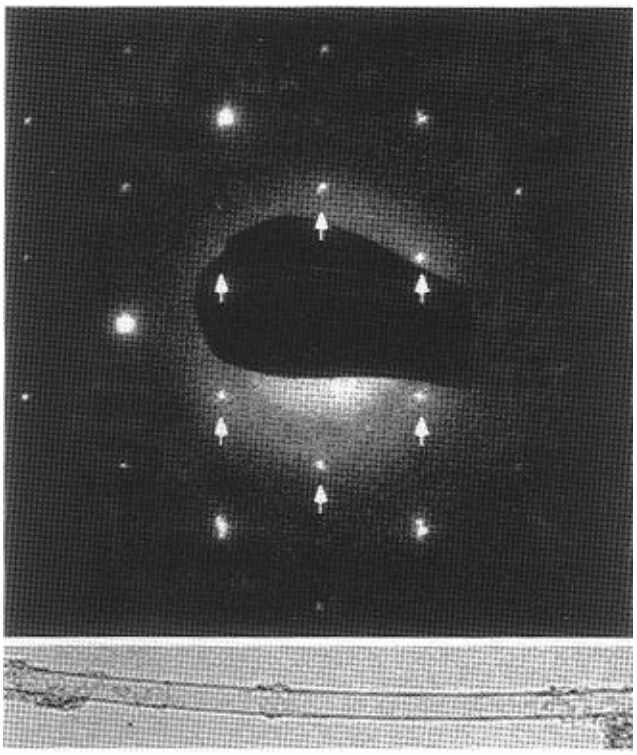

Figure 1. Diffraction pattern and image of a single-layer nanotube with diameter 3.6 nm. The pattern shows the tube has a nonhelical armchair structure.

unchanged for the entire segment of the tube seen in the image. This is in contrast to bends in multilayer tubes, which usually contain pentagon or heptagon defects and changes in the tube diameter.[20] The origin of the change of diameters of multilayer nanotubes is believed to be caused by the instability of the arc plasma environment, where fluctuations of the electric field and the densities of carbon vapor and other charged species introduce pentagon and heptagon defects. The constant diameter of single-layer nanotubes suggests that the twisting and folding of the single-layer nanotube was introduced after the tubes were formed, since stress present during the formation process would likely have led to defects that would have changed its diameter.

The ends of the nanotubes are also of interest, for they may contain clues to the tube growth mechanism. We examined TEM images showing the terminations of the catalytically grown single-layer tubes in an effort to gain insight into their formation process. No catalyst particles were found at the free ends of the tubes, and the shapes of the tube ends resemble those found for multilayer tubes.[20,21] Figure 3 shows tube ends closed with single-layer carbon caps. According to Euler's theorem, to close a cylinder consisting of a rolled hexagonal lattice requires six pentagonal rings to be incorporated into the hexagonal network.[22−24] If the graphene sheet is rolled to give a cone rather than a cylinder, a cap with between one and five pentagons is required to close the cone tip, depending on which of the five possible cone opening angles the cone has.[24,25] We have observed single-layer nanotubes closed with both round end caps reflecting different arrangements of the cap pentagons for these catalytically grown tubes (see Figure 3). Similar carbon structures such as carbon fibers growing in the vapor phase are believed to grow by carbon diffusion over the surface of or through the catalyst particles. This model is supported by TEM results that show almost all the tubes terminated with a metal particle comparable in size to the fiber diameter.[26−28] In contrast, single-layer carbon nanotubes do not contain catalyst particles at the tip. The ends of these nanotubes are similar to

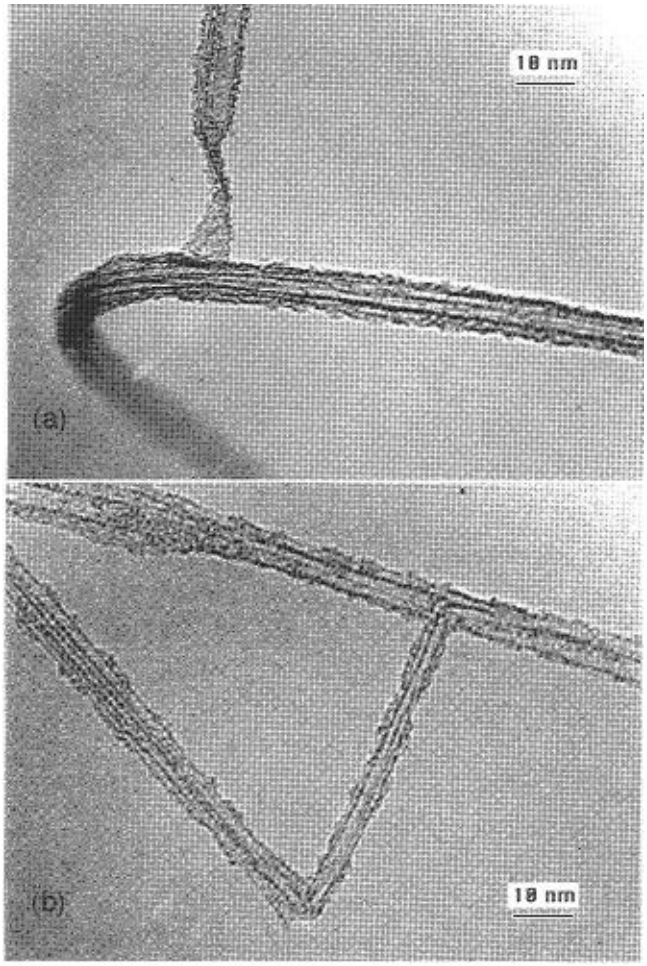

Figure 2. TEM image showing (a) twisting and (b) folding of nanotubes.

the multilayer nanotubes grown on the cathode tip without a catalyst.[21] Therefore, we speculate that the growth of these single-layer nanotubes is similar to the one suggested for tubes grown on the cathode. In this model, nanotubes grow with an open end, and the closure of the tubes is a result of a sudden change of the environment, *e.g.* temperature or carbon vapor density, which causes the formation of pentagons that eventually cap the tube.

4. Effects of Heating the Nanotubes with an Electron Beam

In addition to providing information about the structure of nanotubes, TEM also allows direct observation of the evolution of carbon structures undergoing electron beam irradiation. Electron beam heating has been demonstrated to transform a multilayer nanotube into a nested fullerene cage.[29] Studies of the structural transformation due to local heating of the tubes under vacuum may furnish insight into the self-assembly process that leads to the formation of carbon nanotubes and perhaps fullerenes as well. We observed a variety of nanotube reactions induced by electron beam heating. The most common phenomenon was the development of small ripples in the walls of nanotubes that were initially perfectly straight, and the deformation increased until ultimately the tube broke. The free ends usually reconstructed to form caps (Figure 4, solid arrows), but some of the tubes were left open (Figure 4, hollow arrows). Occasionally the tubes were fragmented into sections, as in the tube in Figure 5, where a 3 nm tube is supporting a 2 nm tube that has been disintegrated into small sections of open cylinders.

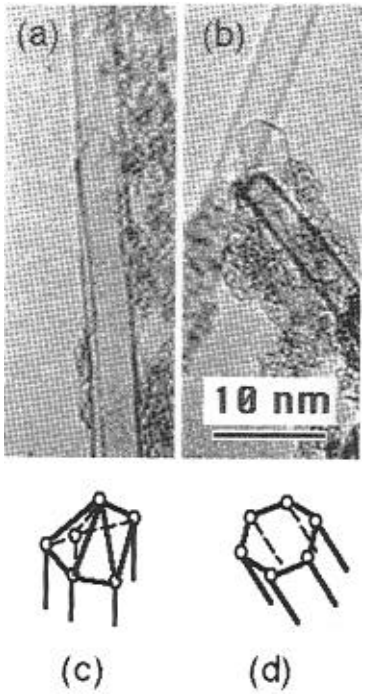

Figure 3. TEM images showing different end cap structures for single-layer nanotubes. The caps are similar to ends typical of multilayer nanotubes. The open circles indicate pentagons. (a) Helical tube capped with six pentagons, as illustrated in part c. (b) Two tubes capped with six pentagons. The nonhelical tube end is illustrated in part d.

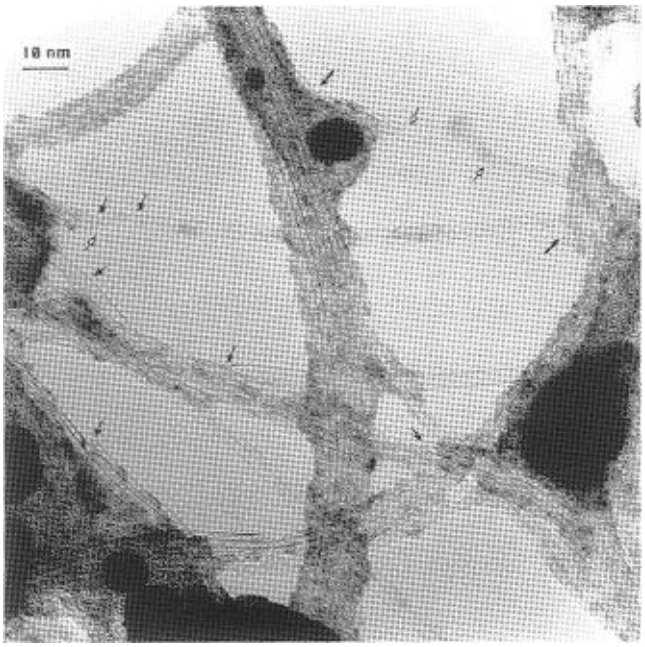

Figure 4. Nanotubes disintegrated under electron beam heating. The arrows point to locations where structural modification occurred due to the electron beam heating. The solid arrows are pointing to closed ends, and the hollow arrows are pointing to open ends of nanotubes.

These segments, if not terminated with an element such as hydrogen, could later reconstruct to form caps to minimized the dangling bonds. Electron beam heating can also be used in a constructive way. We have also observed a tube with a segment that originally had a kink. After one minute of electron beam heating, the kink seemed to be patched, and the tube acquired a regular, cylindrical shape.

How these defects annealed by the electron beam can be rationalized by considering the strain induced by defects in the tube. This strain leads to a structure less stable than one with a perfect hexagonal bonding network. When excess energy is put into the tube, the C−C bonds absorb the energy. They may rearrange, or they may dissociate, causing deterioration of the tube or evaporation of excess carbon. The choice between destruction and reconstruction depends on the dynamics of the heat distribution and bond rearrangement. It also depends on the difference between the heat required for destruction and the barriers to reconstruction. Annealing of nanotubes is expected to result in a structure of lowest energy, which comprises mainly hexagons, as suggested by molecular dynamics simulations.[30] The commonly observed heating effect, which usually results in breaking and capping of nanotubes, is perhaps due to the lack of quenching agent under vacuum in the electron microscope.

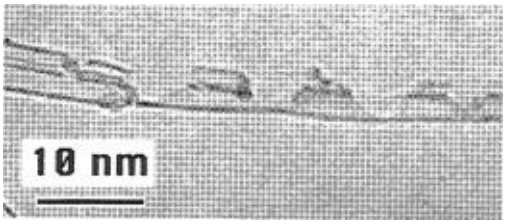

Figure 5. Breaking carbon bonds of single-layer nanotubes under electron beam heating. Two tubes were broken into sections.

We also observed bundling of nanotubes in real time. Parts a−c of Figure 6 are a series of images of a tube taken at approximately 1 min intervals. A tube was initially bridging between two bundles of nanotubes (labeled **A** and **B**). After being heated for one minute, bundle **A** disintegrated, and the bridging tube was separated from it. This tube then slowly moved toward bundle **B**, finally merging with it. Note that it took about 2 min for the tube to sweep across the 20 nm distance. This is an exceptionally long time for such a microscopic motion. It is usually assumed that van der Waals forces are responsible for the assembly of nanotube bundles,[31] with the tubes progressively zipping together. The extremely slow event shown in Figure 6, however, appears not to be explainable by van der Waals or electrostatic attraction. One possibility is that the presence of other materials in the soot could hinder the aggregation of the tubes. It is conceivable that such material could block the aggregation of tubes, causing them to stay apart. We can see from Figure 6a−c that, while imaging the tubes with the electron beam, bundle **A** and the soot near the root of the tube were gradually disintegrated, apparently making it possible for the bridging tube to move and coalesce with bundle **B**. Therefore, a plausible explanation for the slowness of the reaction is that the electron beam irradiation slowly removes material that is blocking the tube aggregation, and the reaction rate is controlled by the rate of evaporation or decomposition of this material.

The use of an electron beam to both induce and view the reaction enables us to study reactions *in situ* and in real time. The effects of heating could be utilized to generate various rearrangements of nanotubes that may be worth investigating. For example, under appropriate conditions the defects in the tubes might be repaired by a suitable dose of irradiation, possibly strengthening the materials. Moreover, breakage and reconstruction of the tubes modifies the morphology of the soot. This could result in a material phase transition from, for example, rubber to glass or crystal.

5. Conclusions

We have produced single-layer carbon nanotubes by co-condensation of arc-vaporized carbon and metal and studied their

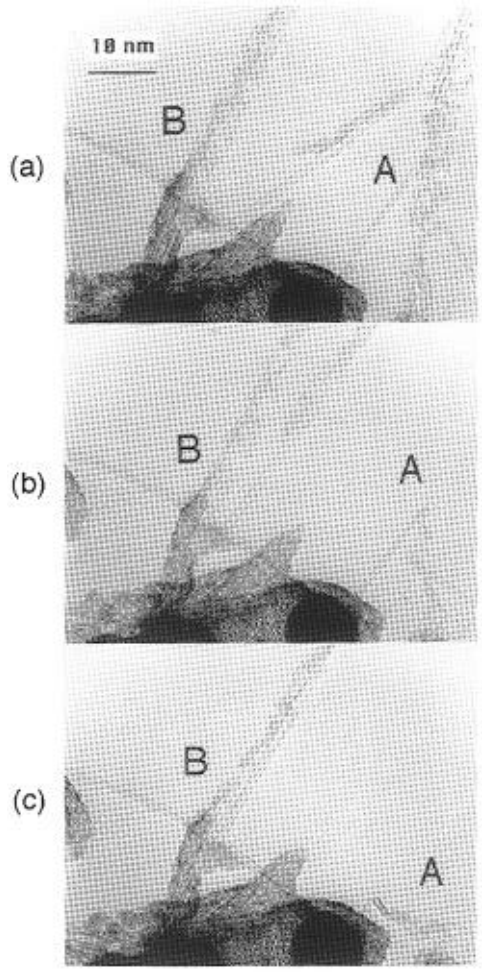

Figure 6. Nanotube bundling imaged in real time. (a) A nanotube bridging between bundles **A** and **B**. (b) Bundle **A** disintegrated, and the tube is pulled toward bundle **B**. (c) The tube eventually merges with bundle **B**.

structure and properties with transmission electron microscopy. The morphology of the catalytically produced nanotubes is different from that of tubes grown on the cathode tip, although the cap structures at the ends of single-layer nanotubes are similar to those of multilayer nanotubes. The detailed atomic structures of single-layer nanotubes can be obtained by electron diffraction, despite the extremely weak diffraction from these novel structures and the limitation on data acquisition time imposed by their susceptibility to electron beam damage. Nanotube structural transformations induced by electron beam heating were found to be either destroyed or repaired, depending on the conditions. Bundling of nanotubes was also observed in real time. The times over which these various transformations occurred ranged from a few seconds to minutes, very slow for molecular motions. We demonstrated opening, closing, and bundling of nanotubes by electron beam heating, which may prove to be a useful approach to modification of these materials on the molecular scale.

Acknowledgment. This research was partially supported by the NSF (Grant ASC-9217368) and by the Materials and Process Simulation Center.

References and Notes

(1) See the papers in the special issue on carbon nanotubes: Iijima, S., Endo, M., Eds. *Carbon* **1995**, *33*.
(2) Iijima, S. *Nature* **1991**, *354*, 56.
(3) Iijima, S.; Ichihashi, T. *Nature* **1993**, *363*, 603.
(4) Bethune, D. S.; Kiang, C.-H.; de Vries, M. S.; Gorman, G.; Savoy, R.; Vasquez, J.; Beyers, R. *Nature* **1993**, *363*, 605.
(5) Kiang, C.-H.; Goddard, W. A., III; Beyers, R.; Salem, J. R.; Bethune, D. S. *J. Phys. Chem.* **1994**, *98*, 6612.
(6) Kiang, C.-H.; Goddard, W. A., III; Beyers, R.; Bethune, D. S. *Carbon* **1995**, *33*, 903.
(7) Kiang, C.-H.; Goddard, W. A., III; Beyers, R.; Salem, J. R.; Bethune, D. S. *J. Phys. Chem. Solids* **1996**, *57*, 35.
(8) Saito, R.; Fujita, M.; Dresselhaus, G.; Dresselhaus, M. S. *Mater. Sci. Eng.* **1993**, *B19*, 185.
(9) Mintmire, J. W.; Robertson, D. H.; White, C. T. *J. Phys. Chem. Solids* **1993**, *54*, 1835.
(10) Saito, R.; Fujita, M.; Dresselhaus, G.; Dresselhaus, M. S. *Phys. Rev.* **1992**, *B46*, 1804.
(11) Dresselhaus, M. S.; Dresselhaus, G.; Saito, R. *Solid State Commun.* **1992**, *84*, 201.
(12) Jishi, R. A.; Inomata, D.; Nakao, K.; Dresselhaus, M. S.; Dresselhaus, G. *J. Phys. Soc. Jpn.* **1994**, *63*, 2252.
(13) Hamada, N.; Sawada, S.-I.; Oshiyama, A. *Phys. Rev. Lett.* **1992**, *68*, 1579.
(14) Jishi, R. A.; Dresselhaus, M. S. *Phys. Rev.* **1992**, *B45*, 11305.
(15) Jishi, R. A.; Venkataraman, L.; Dresselhaus, M. S.; Dresselhaus, G. *Chem. Phys. Lett.* **1993**, *209*, 77.
(16) Fowler, P. W. *J. Phys. Chem. Solids* **1993**, *54*, 1825.
(17) Zhang, X. F.; Zhang, X. B.; Van Tendeloo, G.; Amelinckx, S.; Op de Beeck, M.; Van Landuyt, J. *J. Cryst. Growth* **1993**, *130*, 368.
(18) Robertson, D. H.; Brenner, D. W.; Mintmire, J. W. *Phys. Rev.* **1992**, *B45*, 12592.
(19) Overney, G.; Zhong, W.; Tomanek, D. *Z. Phys.* **1993**, *D27*, 93.
(20) Iijima, S.; Ichihashi, T.; Ando, Y. *Nature* **1992**, *356*, 776.
(21) Iijima, S.; Ajayan, P. M.; Ichihashi, T. *Phys. Rev. Lett.* **1992**, *69*, 3100.
(22) de Wit, R. *J. Appl. Phys.* **1971**, *42*, 3304.
(23) Ajayan, P. M.; Ichihashi, T.; Iijima, S. *Chem. Phys. Lett.* **1993**, *202*, 384.
(24) Iijima, S. *Mater. Sci. Eng.* **1993**, *B19*, 172.
(25) Ge, M.; Sattler, K. *Chem. Phys. Lett.* **1994**, *220*, 192.
(26) Endo, M. *Chemtech* **1988**, *18*, 568.
(27) Tibbetts, G. G. *Carbon* **1989**, *27*, 745.
(28) Baker, R. T. K. *Carbon* **1989**, *27*, 315.
(29) Ugarte, D. *Nature* **1992**, *359*, 707.
(30) Maiti, A.; Brabec, C. J.; Roland, C. M.; Bernholc, J. *Phys. Rev. Lett.* **1994**, *73*, 2468.
(31) Ruoff, R. S.; Tersoff, J.; Lorents, D. C.; Subramoney, S.; Chan, B. *Nature* **1994**, *364*, 514.

JP952636W